

Vibrational energy transfer in CH₄ plasma

T. Butterworth^{1(a)}, A.v.d. Steeg¹, D. v.d. Bekerom¹, T. Minea¹, Q. Ong¹ and G. van Rooij¹

¹ Dutch Institute for Fundamental Energy Research (DIFFER), De Zaale 20, Eindhoven, 5612 AJ, The Netherlands

^aNew author affiliation: King Abdullah University of Science and Technology (KAUST), Clean Combustion Research Centre (CCRC), Thuwal 23955, Saudi Arabia

Abstract:

Plasma generated vibrationally excited CH₄ could be utilised for the selective and efficient production of ethylene. For the first time, using Raman scattering, direct evidence of vibrational non-equilibrium in CH₄ is presented. We study the creation and loss of this vibrationally excited CH₄, as well as the energy transfer processes occurring in the plasma. Using a detailed analysis of the Raman spectra and drawing on literature values, the measured equilibration times are attributed to VT relaxation and fast VV-relaxation.

Keywords: Methane, vibrational excitation, microwave, Raman, Thomson

1. Introduction

Selective direct conversion of methane to ethylene is a “holy grail” of the petrochemical industry. It has been the subject of over 30 years of research, primarily focussed on catalysis. The reaction is thermodynamically limited, since the high temperatures required for a significant conversion of CH₄ also tend to lead to coke formation, which blocks catalyst pores and active sites leading to deactivation of the catalyst [1].

Vibrational excitation promoted dissociation of CH₄ could potentially overcome these limitations. Vibrationally excited molecules can facilitate efficient and low temperature dissociation through VV-excitation or catalytic reactions. This potential for reduced temperature reactions would give an additional parameter to steer selectivity in CH₄ reforming, thus promoting ethylene formation whilst avoiding coke. Microwave plasmas are believed to operate in the optimal reduced electric field range to transfer electrical energy into vibrational modes of molecules. Despite this, MW plasma CH₄ experiments conducted to date appear to be primarily controlled by thermal dissociation, with little evidence for vibrational excitation induced chemistry [2].

In this work we report the first direct measurement of vibrational-rotational non-equilibrium in a CH₄ plasma. We explore both the thermal and vibrational equilibration phenomena, giving new insight into the lifetimes and population densities of the vibrationally excited states of methane.

2. Methane vibrations background

Methane has 4 fundamental vibrational modes: the bending modes, ν_2 and ν_4 , a stretching mode, ν_1 , and an asymmetric stretch mode, ν_3 . These vibrational modes are grouped into “polyads”, represented by P_n , where n is the polyad number, corresponding to vibrational levels with approximately equal energy. The levels of each polyad correspond to the following expression, where the energy of each polyad level is in multiples ~ 1500 cm⁻¹:

$$P_n = 2(\nu_1 + \nu_3) + \nu_2 + \nu_4$$

Throughout this work (e.g. fig. 7) vibrational states are given in the format:

$$[\nu_1, \nu_2, \nu_3, \nu_4]$$

3. Method

CH₄ (99.995%) is fed into a 26 mm diameter, cylindrical quartz tube reactor at a flow of 4 SLM and pressure of 25 mBar. The plasma volume is contained within a WR340 guide, giving a plasma length of up to 34 mm. Assuming ideal plug flow behaviour this flowrate and plasma length limits residence times (t_{res}) to 1 – 5 ms. Plasma ignition is induced repetitively by applying a 200 μ s, 700 W pulse of microwave power at a repetition frequency of 30 Hz, corresponding to a duty cycle of $\sim 0.6\%$, and an interpulse time (t_{int}) of ~ 33 ms. Note that $t_{int} > t_{res}$, meaning that the gas volume is displaced from the reactor before the plasma is reignited. This reignition behaviour is reflected in the power deposition profile, shown in figure 1, and the plasma images shown in figure 2.

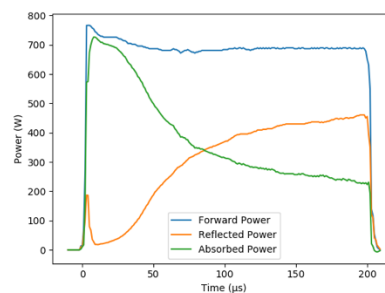


Fig. 1. Power profile of MW pulse in the plasma. Absorbed power in the plasma is forward power minus reflected power.

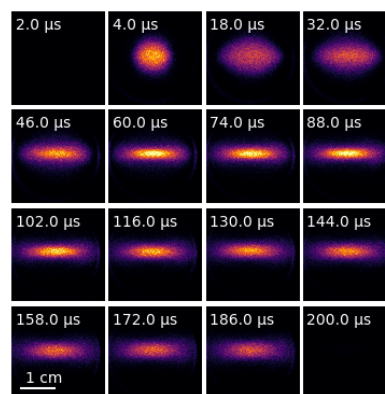


Fig. 2. Light emission (false colour) from the plasma during the 200 μs pulse

Temporally resolved plasma characteristics are determined in-situ using laser scattering techniques: Raman, for vibrational (T_{vib}) and rotational temperature (T_{rot}); and Thomson, for electron density (n_e) and temperature (T_e). A frequency doubled Nd:YAG laser generates a 532 nm focussed beam at 10 Hz, 10 ns pulse duration and an energy of ~ 600 mJ per pulse. The scattered light is coupled via a fireoptic bundle to a 1 m focal length Littrow spectrometer with a 1800 groves / mm grating, giving a spectral resolution of around 0.7 cm^{-1} . The spectrally resolved light is focussed onto an intensified, gated camera (PIMax4 eMCCD).

T_{vib} and T_{rot} are obtained by fitting the CH_4 Raman spectrum in the pentad region at around 3000 cm^{-1} Raman shift. The procedure to fit the Raman spectra is described in detail in [3]. Gas temperature (T_{gas}) can be estimated by integrating the Raman spectrum to obtain the relative CH_4 density, assuming that no CH_4 is converted, the methane temperature is obtained with the ideal gas law. The Thomson scattering spectrum is fit using the assumption of a Maxwellian distribution of the electron energy. This procedure is described in further detail in [4].

4. Results

The temporal evolution of T_{vib} , T_{rot} and T_{gas} during the first 70 μs of the pulse are shown in figure 3. A vibrational-rotational non-equilibrium exists from 10 – 50 μs . During which the strongest non-equilibrium occurs at 20 μs , where $T_{\text{vib}} = 690 \text{ K}$, and $T_{\text{rot}} = 320 \text{ K}$. Equilibration (i.e. $T_{\text{vib}} = T_{\text{rot}} = T_{\text{gas}}$) occurs at 50 μs , where the temperature is 900 K. Beyond this, gas temperature continues to increase beyond 1500 K, at which point the Raman scattering diagnostic is no longer valid to obtain T_{rot} and T_{vib} . It is therefore not possible to obtain temperature measurement further into the pulse.

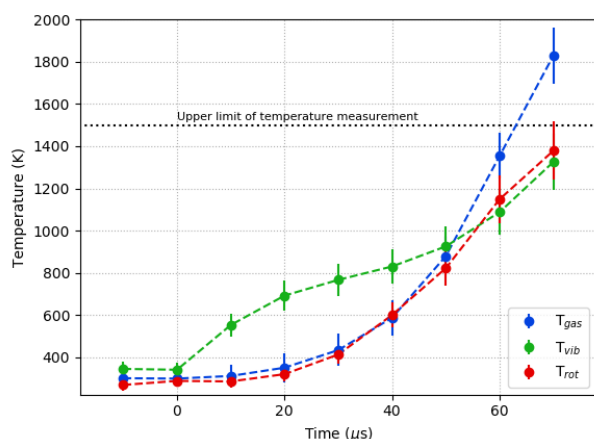


Fig. 3. Vibrational-rotational non-equilibrium occurring during the first 70 μs of MW plasma ignition. N.B. T_{gas} is obtained from the CH_4 density via the ideal gas law. CH_4 conversion can also decrease the measured density and

leads to the difference between T_{gas} and T_{rot} observed from 50 μs onwards.

In this work, we aim to determine the dominant processes that cause the increase in temperature of T_{rot} and T_{gas} on the short timescales observed. We also wish to know: Is it possible to extend the timescales before thermal equilibration occurs? Is the increase in T_{rot} due to VT relaxation, or some other avoidable mechanism? What does it mean to have a vibrational temperature of 700K in CH_4 ? Can we exploit the vibrational non-equilibrium for useful chemical reactions?

In order to determine how the non-equilibrium is established and the processes that lead to the subsequent equilibration it is important to know into which degrees of freedom the power being applied to the plasma is deposited. This power deposition fraction can be either derived from the vibrational and rotational temperature measurements, or derived from CH_4 electron collision cross sections (using Bolsig+) and cross referencing the experimentally measured electron temperatures.

T_e derived power partition

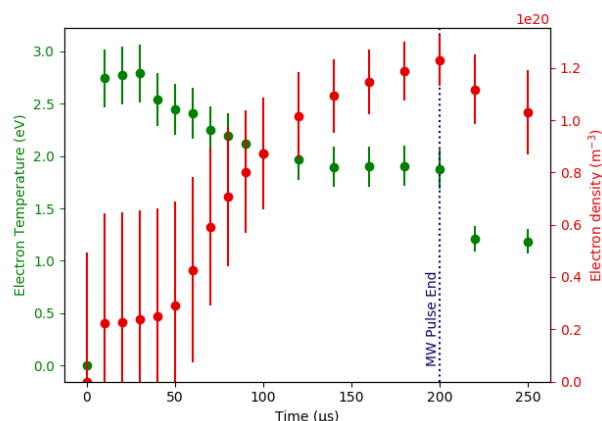


Fig 4. Electron temperature is high (2.7 eV) during plasma ignition and drops towards 1.9 eV as the electron density increases.

Figure 4 shows the temporal evolution of n_e and T_e during the 200 μs plasma pulse. For the first 30 μs , T_e is at a maximum, having a value of $2.7 (\pm 0.25) \text{ eV}$. As the plasma progresses the electron temperature approaches a plateau at 1.9 eV from $\sim 140 \mu\text{s}$ until the end of the pulse, where T_e drops sharply.

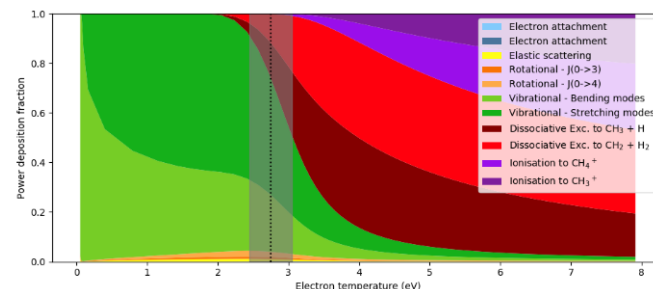


Fig. 4. At 2.7 eV, 70 (± 20)% of the input power is transferred to bending and stretching vibrational modes of CH₄. Calculated using Bolsig+ with data from IST Lisbon data set from LXCat.

The electron derived power partition as a function of the electron temperature is shown in figure 4. 2. $T_e = 2.7$ eV, corresponding to the 20 μ s measurement is marked by the black dashed line on the plot. At this electron temperature, the calculated power deposition reveals that between 50 – 90% of the energy is deposited into vibrational modes of CH₄. Of that vibrational power deposition, the power fraction in the stretching modes (ν_1 and ν_3) is approximately twice that of the bending modes (ν_2 and ν_4). Note that the one quantum of energy in ν_1 or ν_3 (~ 0.36 eV), is about twice that in ν_2 or ν_4 (~ 0.18 eV). Therefore the rate of populating bending and stretching vibrational modes is approximately equal.

Temperature derived power partition

The temperature derived power partition is obtained from the temperature evolution profiles (in fig. 3.) together with the power deposition (fig. 1.) and plasma images (fig. 2.). The power deposition fraction during the pulse is shown in figure 5.

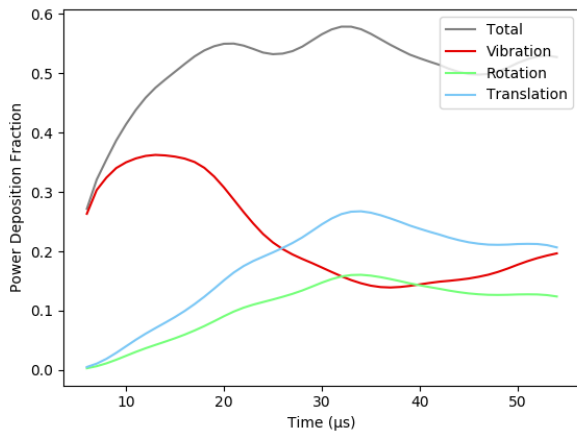


Fig. 5. Temperature derived power partition fraction.

At 10 – 20 μ s into the pulse, 35 (± 15)% of the input energy is deposited into CH₄ vibrational modes. Following this the power deposition into vibrations decreases to around 20%, whilst power to rotation and translation increases. Considering the assumptions and contributing errors, this 35% fraction to vibration is in a reasonable agreement with the electron based power partition obtained from the T_e data and Bolsig calculation.

As the plasma develops following ignition, the electron temperature begins to drop. As this occurs, the power deposition into vibrational modes should be increasing, however, we observe the opposite occurring; the vibrational power fraction decreases whilst rotational and translational power fraction increases. This indicates that either less power is deposited into vibrations, or that energy

deposited into vibration, electronic excitation or ionisation is transferred into rotation and translation. Based on the data in fig 1 - 5, it is not possible to determine the dominant energy transfer mechanism to rotation and translation. However, a number of infrared laser studies report vibrational relaxation times in CH₄. VT relaxation times from the 1st bending mode vibrational levels are approximately 50 μ s (at 300 K and 25 mBar). This is remarkably similar to the measured equilibration timescale, shown in figure 3, and suggests that VT relaxation may be the dominant mechanism.

Electronic excitation and ionisation tend to lead to dissociation of CH₄, which in turn leads to heating through energy redistribution and recombination of nascent CH₄ dissociation fragments. Without a kinetic model we cannot rule out the possibility of this indirect heating mechanism through electronic excitation and ionisation.

Vibrational energy transfer

As described previously, the electron-derived reaction kinetics indicate that the bending and stretching vibrational modes are populated at an equal rate. Therefore, if we assume that these vibrational states are not consumed, the population density of bending and stretching modes should be equal, i.e. 1:1 population density. Conversely, at $T_{\text{vib}} = 690\text{K}$, thermodynamics (Boltzmann distribution) predicts that the ratio of the 1st bending to the 1st stretching mode population density is at least 35:1. Furthermore, there is no equilibrium vibrational temperature where the bending to stretching mode ratio is 1:1. i.e. Ignoring consumption of the vibrational states, plasma kinetics predicts a vibrational-vibrational non-equilibrium that would not be possible with equilibrium thermodynamics.

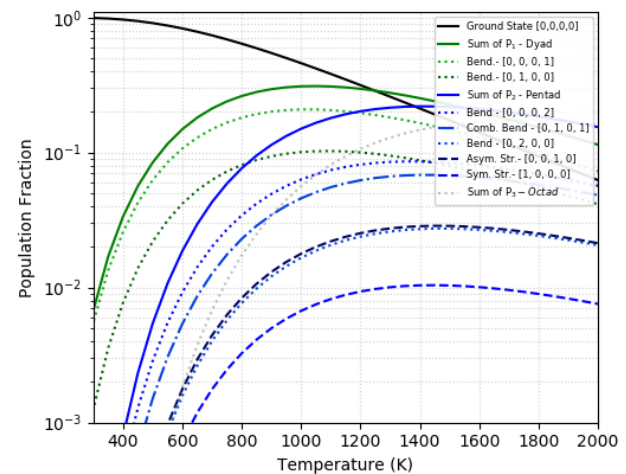


Fig. 6. Calculated thermodynamic population distribution of vibrational states in CH₄ up to the pentad. The format for vibrational modes is [Sym. stretch, Sym. bend, Asym. stretch, Asym. bend]. Dotted lines are bending modes, dashed lines are stretching modes, and the dot-dash line is the combination bending mode.

Raman spectroscopy can be used to directly probe the population density of the CH₄ vibrational states. The fitting algorithm used to obtain T_{vib} and T_{rot} is based on the assumption of a Boltzmann distribution of the vibrational states, and indeed, it returns an excellent fit. This in itself reveals that within the plasma that the vibrational distribution is close to the thermodynamic distribution, rather than a plasma kinetic induced vibrational non-equilibrium.

Figure 7 shows the Raman spectrum recorded at 20 μs, together with the calculated fit for T_{vib} and T_{rot}, as well as the vibrational states that contribute to the recorded spectrum.

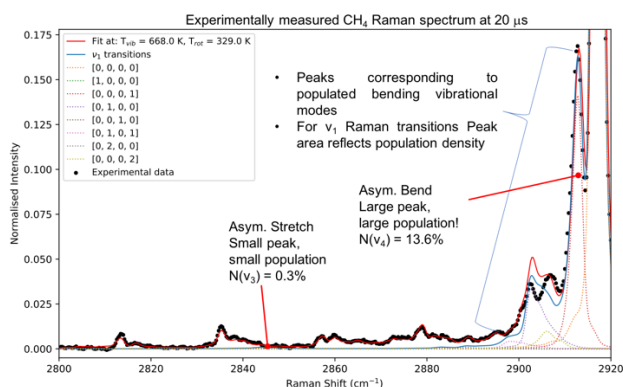


Fig. 7. The CH₄ Raman spectrum in the Pentad region. The asymmetric stretch and asymmetric bend peaks are highlighted. Note that the area of the peaks approximately reflects the population density of the vibrational state, provided that they correspond to the same Raman transition (in this case, $\Delta v_1 = 1$).

If the asymmetric stretch mode was similarly populated to the bending mode it would be clearly visible in the Raman spectrum, yet it is not. The Raman spectrum reveals that the vibrational level population can be (almost) predicted with a Boltzmann distribution.

Why is it that the asymmetric stretch mode does not have a large population density as predicted by the electron kinetics? This can be attributed to the very fast relaxation that occurs between vibrational levels in the same polyad. Literature values obtained from IR laser excitation experiments suggest that at the experimental conditions tested (25 mBar), relaxation occurs on 10 – 50 ns timescales. I.e. vibrational-vibrational relaxation leads to fast depletion of the stretching modes and a thermodynamic distribution of vibrational states being established. This has important implications for the plasma conversion and plasma catalysis communities as it imposes a temporal and spatial constraint on the population density of CH₄ in the stretching vibrational modes.

5. Conclusion

For the first time we present direct evidence of a vibrational non-equilibrium in a CH₄ plasma. This non-

equilibrium is sustained for 50 μs, before thermal equilibrium is re-established at approximately 900 K. From analysis of the temporal evolution of the plasma parameters, and drawing on pre-existing literature from IR excitation experiments, there is compelling evidence to suggest that the dominant energy transfer mechanism to rotational and translational degrees of freedom is VT-relaxation. I.e. The VT relaxation rate imposes the limits on the vibrational non-equilibrium timescales observed. However, it is also possible that vibrational excitation is effective at the fast time scales to assist in higher energy processes (electronic excitation and ionisation).

Furthermore, based on the CH₄ Raman spectrum we observe that the vibrational levels follow a Boltzmann distribution, rather than a vibrational-vibrational non-equilibrium that would be expected based on the electron kinetics. This is attributed to relaxation between vibrational levels occurring on 10s of nanosecond timescales.

6. Acknowledgments

T. Butterworth would like to acknowledge financial support received from Shell Global Solutions International. Thank you also to S. van Bavel, J. Smits, and C. van Kruijsdijk for your continued input and direction.

7. References

- [1] P. Schwach; X. Pan; X. Bao; Chemical Reviews, **117**, (2017)
- [2] T. Minea; D. v.d. Bekerom; F. Peeters; E. Zoethout; M. Graswinckel; M v.d. Sanden; T. Cents; L Lefferts; G. J. v. Rooij. Plasma processes and polymers, **15**, 11 (2018)
- [3] A.v.d. Steeg; T. Butterworth; G. J. van Rooij. *Vibrational and gas heating dynamics in molecular plasma assessed by Thomson and Raman scattering* (Submitted – ISPC)
- [4] T. Butterworth; B. Amyay; D. v.d. Bekerom; A. v.d. Steeg; N. Gatti; Q. Ong; C. Richard; V. Boudon; C. van Kruijsdijk; J. Smits; S. v. Bavel; G. J. van Rooij. *Quantifying methane vibrational and rotational temperature with Raman scattering* (Submitted)